RESEARCH ARTICLE

WILEY

Trace residue identification, characterization, and longitudinal monitoring of the novel synthetic opioid β-U10, from discarded drug paraphernalia

Henry West[1] | John L. Fitzgerald[2] | Katherine L. Hopkins[1,2] |
Michael G. Leeming[3] | Matthew DiRago[4,5] | Dimitri Gerostamoulos[4,5] |
Nicolas Clark[6,7] | Paul Dietze[8,9] | Jonathan M. White[1] | James Ziogas[10] |
Gavin E. Reid[1,10,11]

[1]School of Chemistry, The University of Melbourne, Parkville, Victoria, Australia

[2]School of Social and Political Science, The University of Melbourne, Parkville, Victoria, Australia

[3]Melbourne Mass Spectrometry and Proteomics Facility, Bio21 Molecular Science and Biotechnology Institute, The University of Melbourne, Parkville, Victoria, Australia

[4]Victorian Institute of Forensic Medicine, Southbank, Victoria, Australia

[5]Department of Forensic Medicine, Monash University, Clayton, Victoria, Australia

[6]North Richmond Community Health, Richmond, Victoria, Australia

[7]Addiction Medicine Service, Royal Melbourne Hospital, Parkville, Victoria, Australia

[8]National Drug Research Institute and enAble Institute, Curtin University, Melbourne, Victoria, Australia

[9]Disease Elimination Program, Burnet Institute, Melbourne, Victoria, Australia

[10]Department of Biochemistry and Pharmacology, The University of Melbourne, Parkville, Victoria, Australia

[11]Bio21 Molecular Science and Biotechnology Institute, The University of Melbourne, Parkville, Victoria, Australia

Correspondence
Gavin E. Reid, School of Chemistry, The University of Melbourne, Parkville, Victoria 3010, Australia.
Email: gavin.reid@unimelb.edu.au

Funding information
Victoria State Government Department of Health

Abstract

Empirical data regarding dynamic alterations in illicit drug supply markets in response to the COVID-19 pandemic, including the potential for introduction of novel drug substances and/or increased poly-drug combination use at the "street" level, that is, directly proximal to the point of consumption, are currently lacking. Here, a high-throughput strategy employing ambient ionization-mass spectrometry is described for the trace residue identification, characterization, and longitudinal monitoring of illicit drug substances found within >6,600 discarded drug paraphernalia (DDP) samples collected during a pilot study of an early warning system for illicit drug use in Melbourne, Australia from August 2020 to February 2021, while significant COVID-19 lockdown conditions were imposed. The utility of this approach is demonstrated for the de novo identification and structural characterization of β-U10, a previously unreported naphthamide analog within the "U-series" of synthetic opioid drugs, including differentiation from its α-U10 isomer without need for sample preparation

or chromatographic separation prior to analysis. Notably, β-U10 was observed with 23 other drug substances, most commonly in temporally distinct clusters with heroin, etizolam, and diphenhydramine, and in a total of 182 different poly-drug combinations. Longitudinal monitoring of the number and weekly "average signal intensity" (ASI) values of identified substances, developed here as a semi-quantitative proxy indicator of changes in availability, relative purity and compositions of street level drug samples, revealed that increases in the number of identifications and ASI for β-U10 and etizolam coincided with a 50% decrease in the number of positive detections and an order of magnitude decrease in the ASI for heroin.

KEYWORDS
DART, mass spectrometry, novel synthetic opioid, trace residue analysis, β-U10

1 | INTRODUCTION

To date, studies to examine changes to the illicit drug market during the current COVID-19 pandemic have largely been focused on monitoring population level trends associated with known drug substances via wastewater analysis,[1–3] by conducting surveys of people who use drugs,[4] and inferences from secondary indicators of drug-related harms.[5] Therefore, empirical data regarding the potential for dynamic alterations in drug availability or purity, increased adulteration or poly-drug use, or the introduction of novel drug substances at the "street" level, that is, directly proximal to the point of consumption, are currently lacking. The potential for introduction of new psychoactive substances (NPS) or adulterants into the illicit drug market, including novel synthetic opioids (NSOs), is of particular concern due to their often poorly understood pharmacological properties and potential for higher potencies compared with traditional opioid drugs (e.g., heroin, oxycodone, etc.).[6–9] For example, in addition to the well-known fentanyl and fentanyl-analog phenylpiperidine opioid drugs, a lesser known class of NSO's include the "AH-" (e.g., AH-7921), and "U-" series of benzamide (e.g., U-47700) and acetamide (e.g., U-50488) drugs. U-47700 is a potent μ-opioid receptor agonist, reported to be 7.5 times more potent than morphine (in animal models), while U-50488 is a κ-opioid receptor agonist.[6] Originating from the Allen and Hanburys[10,11] and Upjohn Companies[12] in the 1970s, the AH- and U-series of drugs have never been brought to market for therapeutic use but have increasingly appeared in the illicit drug market since the early 2010s, with numerous fatalities reported worldwide.[6,8,13–16]

Predominately, newly emerging NSO's are identified and characterized from intact samples seized by law enforcement agencies,[17] obtained during online monitoring of drug markets,[18] or provided by individuals presenting for medical care after experiencing adverse effects following consumption,[19] using a range of analytical chemistry techniques including Fourier-transform infrared spectroscopy (FT-IR), gas chromatography–mass spectrometry (GC–MS), and liquid chromatography (LC–MS) using electrospray ionization (ESI), LC tandem mass spectrometry (MS/MS), and nuclear magnetic resonance (NMR). The

sensitivity of GC–MS and LC–MS and –MS/MS methods also facilitate the use of these techniques for trace residue analysis of the contents of discarded drug paraphernalia (DDP), such as used syringes, where materials may be present in only microgram to nanogram quantities.[20–25] These later efforts can provide information on the prevalence of specific drug substances, adulterants, and poly-drug combinations that are in use within a specific population at the end of the supply chain and proximal to the site of consumption. However, as these methods typically use "targeted" approaches for detection and also require relatively long time frames for sample preparation and analysis that limits the scale at which they can be applied (e.g., for large-scale monitoring applications), the emergence of newly emerging NSO drugs that initially are not in widespread use within a given community may potentially go undetected.[26,27]

As an alternative, a range of MS-based "ambient" ionization techniques that require minimal sample preparation and with capability for higher throughput compared to GC– and LC–MS have recently been developed and applied to the trace residue analysis of illicit drug substances, including those present in biofluids (saliva, urine, blood etc.) and DDP. Examples include desorption electrospray ionization (DESI),[28–30] paper-spray (PS),[31–33] low-temperature plasma (LTP) ionization,[34] atmospheric solids analysis probe (ASAP),[35] and direct analysis in real time (DART).[36–40] When coupled with high-resolution accurate mass spectrometry and MS/MS techniques, the identification and characterization of unexpected or novel drug substances may potentially be achieved using these approaches, via assignment of the molecular formulae of the observed ions and by similarities in MS/MS fragmentation behavior compared with structurally homologous known substances within an established drug class.[41–44]

Recently, we described the development and application of a DART-MS and -MS/MS approach for rapid and high-throughput trace residue sampling and analysis of discarded drug packaging samples (DPS) as part of an early warning monitoring system for illicit drug use at large public events. This approach was shown to be applicable for the identification and characterization of a wide range of illicit drugs and adulterant substances, including numerous NPS and complex poly-drug mixtures, using laboratory-based instrumentation as well as

in "close-to-real-time" applications using a transportable mass spectrometer housed within a mobile analytical laboratory.[40] Here, we describe the extension of this approach for the identification of substances present within >6,600 DDP samples collected during a 6-month pilot study between September 2020 and February 2021 in Melbourne, Australia, while significant COVID-19 lockdown conditions were in place. Notably, this enabled the de novo identification and structural characterization of a previously unreported naphthamide analog within the "U-series" of NSO drugs, namely, β-U10, that was observed in over 800 samples and in temporally distinct clusters throughout the study. Furthermore, we also report the development of a semi-quantitative strategy for longitudinal monitoring of the number and weekly average signal intensity (ASI) of identified substances, including β-U10, as a proxy for changes in the availability, relative purity, and compositions of "street-level" drug samples.

2 | MATERIALS AND METHODS

2.1 | Chemicals and reagents

1-Naphthyl chloride, 2-naphthyl chloride, LC–MS grade dichloromethane, LC–MS grade ethyl acetate, methanol, sodium sulfate, sodium hydroxide, and triethylamine were purchased from Sigma-Aldrich (Castle Hill, NSW, Australia). (1R,2R)-N,N,N'-trimethyl-1,2 diaminocyclohexane was purchased from BLD Pharmtech Ltd (Shanghai, China). Cotton tip applicators were purchased from Swisspers (Kingsgrove, NSW).

2.2 | DDP sample collection and preparation

DDP consisting of used 1 mL, 3 mL, and other volume syringes, plastic spoons, and aluminum trays and DPS including disposable plastic ziplock bags, aluminum foil, plastic wrap, and other items were collected once weekly (estimated number of 500–1,000 items total per week) from established service providers across metropolitan Melbourne, Victoria, Australia, during a 24-week pilot study from August 2020 to February 2021 (20 weeks from August 3, 2020 to December 11, 2020 and another 4 weeks from January 11, 2021 to February 5, 2021). This period of time coincided with a strict lockdown imposed across metropolitan Melbourne from August 2, 2020 to October 18, 2020 due to the COVID pandemic,

which included a 2-h daily time limit for outdoor activities, a 5-km (3.1 mile) radius restriction on outdoor movement from the primary residence, and a night time curfew from 8 p.m. to 5 a.m. This was followed by a series of stepwise relaxation of restrictions until November 8, 2020, after which travel was allowed to and from anywhere in the state. From approximately 500–1,000 DDP collected each week, an average of 276 per week were selected for analysis (6,631 samples total, Table 1).

A syringe decapitator was used to safely remove the needle from syringes, followed by plunger removal and visual inspection. Samples were then prepared for analysis by lightly swabbing the surface area of the DDP (e.g., the inside of the barrel of syringes, the inner surface of plastic spoons or metal trays, or the interior of ziplock bags as previously described[40]) using commercially available cotton tip applicators (Swisspers, Kingsgrove, NSW, Australia). The majority of DDP samples contained no visible residue. However, for samples containing visible residue, the cotton tip applicators were gently flicked after swabbing to displace any loose material. Samples containing blood, saline, or other liquids were swabbed and then allowed to dry prior to analysis.

2.3 | DART-MS and MS/MS of DDP samples

Samples were introduced to a Thermo Scientific Q Exactive Plus (Bremen, Germany) mass spectrometer using a DART source and a Vapur Interface (IonSense, MA, USA), as previously described.[40] The probe heater was set to 200°C using nitrogen as the ionizing gas. Swabs were positioned between the probe and the Vapur interface using a probe position setting of 6 (arbitrary value). The transfer capillary temperature of the mass spectrometer was set to 250°C. Ultrahigh-resolution/accurate mass spectra (UHRAMS) were acquired over a range of m/z 100–500 in positive ionization mode. Higher energy collision-induced dissociation (HCD)-MS/MS spectra were acquired using an isolation window of ±0.5 or 1 m/z, with a normalized collision energy set between 10% and 40% depending on the precursor ion of interest. For both MS and MS/MS experiments, ions were detected using the Orbitrap mass analyzer operating with a mass resolving power of 17,500 (at 200 m/z) and an AGC target of 1.0E6. Spectra were averaged across 100 scans with MS data collected in 6 s and HCD-MS/MS in 10 s. Blank cotton swabs were run every five samples as controls.

TABLE 1 Summary of the number and type of DDP samples analyzed during this study

Syringe (1 mL)	Syringe (3 mL)	Syringe (other vol.)	Plastic spoon	Metal tray	DPS[a]	Other[b]	Total
4,738	781	21	341	221	494	35	6,631
71.5%	11.8%	0.3%	5.1%	3.3%	7.5%	0.5%	

[a]DPS as defined in West et al.[40]
[b]Samples categorized as "other" included glass "pipes", glass ampules, and teaspoons.

2.4 | Data analysis, identification, and semi-quantitative ASI calculations

A database of illicit drug substances, known adulterants, bulking agents, and common contaminants was compiled (over 1,000 substances in total at the time of writing, and regularly updated as new substances are reported in both the literature and publicly available databases including NPS discovery[45]), along with the exact m/z values for their $[M + H]^+$ ions. Thermo ".raw" files produced by DART-MS analysis were first converted to ".mzML" format using msconvert[46] (v3.0.21040.fbf7857be) with vendor-specific peak centroiding activated. Individual mass spectra were then accessed using a Python (v3.7.5) script developed in-house, using the pymzML[47] (v2.4.7) library and the summed intensities of ions within ±5 ppm of the theoretical $[M + H]^+$ m/z value of each substance in the database were extracted. Given that the total ion current (TIC) of individual spectra acquired from each sample using DART often varied substantially over the acquisition period, individual spectra with the lowest 50% TIC were first excluded, then target abundances were computed by averaging the signal intensities from the remaining spectra. The Python scripts used for processing are available from the authors upon request. Positive identifications were assigned only if the signal intensity for the precursor ion of interest was greater than the limit of detection (defined as the mean + 3 times the standard deviation of the blank) *and* greater than an arbitrary absolute threshold of 1E4, below which high-quality MS/MS spectra for more species could not be acquired for definitive identification. Calculation of weekly ASI values was achieved by averaging the processed signal intensities for the individual substances identified in each sample, from each week of analysis.

2.5 | Synthesis and characterization of α-U10 and β-U10 reference standards

α-U10 and β-U10 reference standards were prepared via reaction of (1R,2R)-N,N,N′-trimethyl-1,2 diaminocyclohexane (500 mg, 3.20 mmol) with 1-naphthoyl chloride and 2-naphthoyl chloride, respectively, then the structures confirmed by X-ray crystallography (Figure S1),[48–50] GC–MS, and LC–MS[27] (see Methods S1 for further details).

2.6 | ESI-HCD-MS/MS and 213-nm UVPD-MS/MS of the m/z 311.21 ion and authentic reference standards

Selected DDP samples containing visible residue extracted into either methanol or water, and the authentic reference standards dissolved in either methanol or water, were introduced to an Orbitrap Fusion Lumos mass spectrometer (Thermo Scientific, San Jose, CA, USA) via direct infusion using a Triversa Nanomate nESI source (Advion, Ithica, NY, USA) operating with an ionization potential of 1.40 kV and gas pressure of 0.30 psi. HCD-MS/MS spectra on the m/z 311.21 precursor ions were acquired using the Orbitrap analyzer operating at a mass resolving power of 17,500 (at 200 m/z) and an AGC target of 100%, over an m/z of 50–350 using an isolation window of ±0.4 m/z and with the normalized collision energy set between 10% and 50%. Two hundred thirteen-nanometers ultraviolet photodissociation (UVPD)-MS/MS spectra were collected using an irradiation time of 100 ms.

2.7 | Ethics and regulatory approvals

This study was approved by the University of Melbourne Human Research Ethics Committee. Approval for the collection, analysis, and storage of the illicit drugs of interest was granted under the terms of a permit to purchase or otherwise obtain poisons or controlled substances for industrial, educational, or research purposes granted to the Bio21 Molecular Science and Biotechnology Institute at the University of Melbourne, under the Drugs, Poisons and Controlled Substances Act 1981 (No. 9719).

3 | RESULTS AND DISCUSSION

3.1 | Trace level DART-MS and -MS/MS analysis of DDP

Throughout the course of this 24-week pilot study, 6,631 DDP samples (an average of 278/week) that were suspected to contain residual drug material were analyzed by DART-MS and -MS/MS. Five thousand seven hundred four (86%) tested positive for at least one cataloged drug substance. Starting the week of September 14, 2020, a prominent but unknown ion at m/z 311.2122 (calc. composition $C_{20}H_{27}N_2O$) was observed in combinations with various known drug substances (Figure 1), that was not observed in the control blank samples. Panel a in Figure 1 shows the spectrum obtained from a plastic spoon, the first sample in which this m/z 311.21 ion was observed, that also tested positive for heroin (calc. m/z 370.1655) and etizolam (calc. m/z 343.0779), a thienodiazepine drug that is not approved for medical use in Australia.[51] Other representative spectra, including from analysis of a plastic 1-mL syringe also containing etizolam and paracetamol (calc. m/z 152.0706), a metal tray also containing heroin, etizolam, cocaine (calc. m/z 304.1549), diphenhydramine (calc. m/z 256.1701), MDMA (calc. m/z 194.1181), and methamphetamine (calc. m/z 150.1283), and a metal tray also found to contain heroin, diphenhydramine, noscapine (calc. m/z 413.1547), papaverine (calc. m/z 340.1543), acetylcodeine (calc. m/z 342.1700), monoacetylmorphine (calc. m/z 328.1543), and xylitol (calc. m/z 153.0788), are shown in Figure 1b–d, respectively. The HCD-MS/MS spectra used to definitely confirm the identity of each of these known substances are shown in Figure S2.

This unknown ion at m/z m/z 311.2122, subsequently identified and characterized as β-U10 (see below), was observed a total of 838 times throughout the course of this study, most commonly in
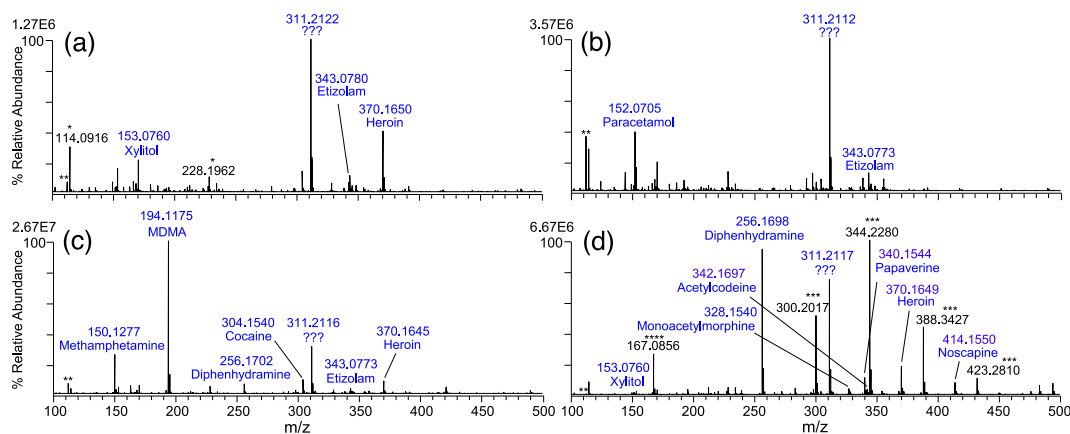
FIGURE 1 DART-UHRAMS trace residue analysis of discarded drug paraphernalia (DDP) containing an unknown ion at m/z 311.2122 (calc. Composition $C_{20}H_{27}N_2O$). Spectra resulting from analysis of (a) a plastic spoon also containing heroin and etizolam, (b) a plastic 1-mL syringe also containing etizolam and paracetamol, (c) a metal tray also containing heroin, etizolam, cocaine, diphenhydramine, MDMA, and methamphetamine, and (d) a metal tray also containing heroin, diphenhydramine, noscapine, papaverine, acetylcodeine, monoacetylmorphine, and xylitol. *background ions. **ammonium ion adduct of dimethylsulfone. ***polyethylene glycol (PEG) polymers arising from the diphenhydramine capsules. ****in-source fragment of diphenhydramine [Colour figure can be viewed at wileyonlinelibrary.com]
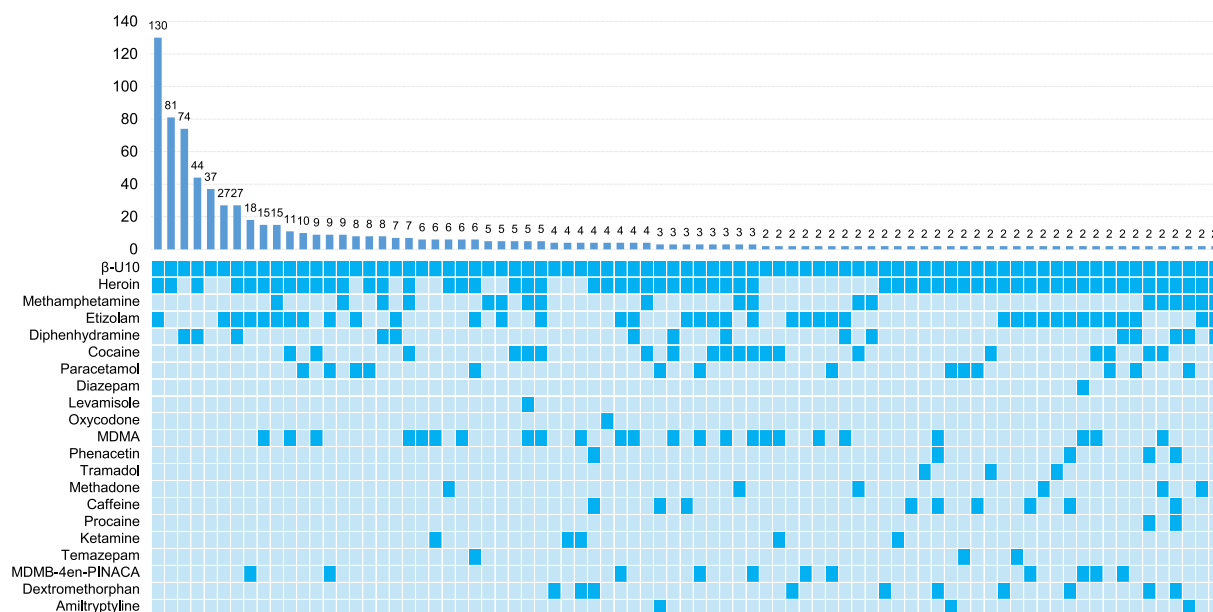

FIGURE 2 Summary of β-U10 drug combinations identified by trace residue DART-UHRAMS analysis, observed in at least two discarded drug paraphernalia (DDP) samples [Colour figure can be viewed at wileyonlinelibrary.com]

combination with (i) heroin and etizolam (130 times), (ii) heroin (81 times), (iii) diphenhydramine (74 times), (iv) heroin and diphenhydramine (44 times), (v) etizolam (27 times), and (vi) heroin, etizolam and diphenhydramine (27 times), and only 37 times on its own. However, these combinations represented only 50% of the samples in which β-U10 was observed, and overall, β-U10 was found in combination with 23 other drug substances in a total of 182 different polydrug combinations containing up to seven additional substances. A matrix plot showing each of the detected drugs, drug combinations, and the number of times each was observed, is shown in Figure 2 for

combinations observed at least twice and in Figure S3 for combinations detected only once.

3.2 | Longitudinal monitoring of weekly drug identifications and ASI values

As the majority of DDP samples containing no visible residue, this study involved trace residue analysis only. Thus, no quantitative information could be obtained regarding the absolute or relative amounts

of β-U10 or other drug substances that were present. However, as a large number of samples were available to be analyzed each week, it was of interest to determine whether changes in the number of detections of a particular drug, or their relative signal intensity in the mass spectra, could potentially serve as proxy indicators of changing market conditions, particularly those that may have occurred in response to COVID lockdown restrictions in Melbourne during the time period when the pilot study was performed. To achieve this, the individual signal intensity of drugs identified in each sample was extracted from the mass spectra then filtered using the procedure described in Section 2 above, prior to averaging the processed signal intensities of all samples in each week of analysis to generate a set of weekly ASI values. For example, plots showing the individual signal intensities and total number of detections for heroin, etizolam, and β-U10 during each week of the pilot study, and their $\log_{10}$ ASI values, are presented in Figure 3.

Notably, a significant decrease in the ASI for heroin was observed starting the week of October 12, before reaching a minimum in the week of November 9 at a level one order of magnitude lower than that seen in the first week of the study (Figure 3a). This was then followed by a gradual increase over several weeks and stabilization, albeit not back to original levels, at the end of the study. Coinciding with this decline in ASI was a >50% decrease in the number of weekly samples that tested positive for heroin. Preceding this decline by several weeks was the onset of the appearance of both β-U10 and etizolam, whose number of detections rapidly increased over several weeks while experiencing relatively constant ASI values, and that overlapped with the decrease in number of identification and ASI for heroin. As the heroin ASI then rebounded, both the number of detections and ASI of β-U10 and etizolam decreased. In contrast, the number of weekly identifications for methamphetamine that was observed in combination with β-U10 only 125 times throughout the study, fluctuated significantly on a weekly basis, but its ASI remained relatively constant (a difference of only threefold was observed over the 24-week pilot) (Figure S4).

3.3 | Trace level de novo structural elucidation and characterization of the m/z 311.21 ion as U10

UHRAMS analysis enabled a molecular formula of $C_{20}H_{25}N_2O$ to be proposed for the m/z 311.2122 ion shown in Figure 1a. HCD-MS/MS spectra of the m/z 311.2122 ion at multiple collision energies were then acquired in an attempt to assign its identity (see Figure 4). However, the experimentally observed fragmentation behavior did not match any available reference MS/MS spectra for substances with the proposed molecular formula. Furthermore, the spectrum was significantly different to that of any of the drug compound classes that had previously been observed in this, or our previous studies.[40] Conventional higher energy collision-induced dissociation (HCD)-MS/MS at low relative collision energy provided only limited structural information, with a single dominant product ion at m/z 266.1532 corresponding to the loss of C_2H_7N: either dimethylamine or
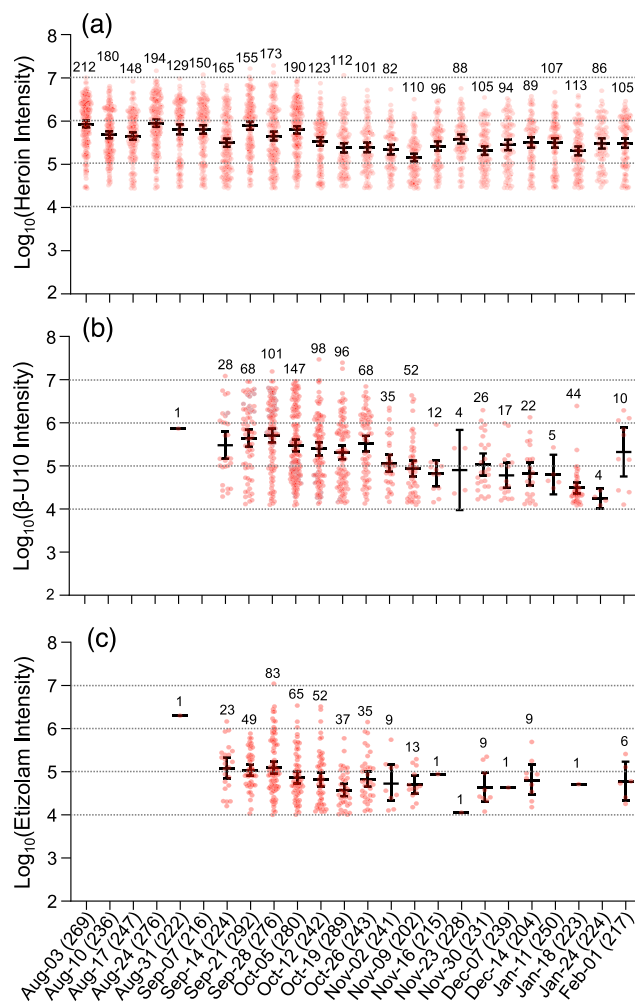

FIGURE 3 Weekly $\log_{10}$ average signal intensity and number of detections for (a) heroin, (b) β-U10, and (c) etizolam. The plot shows the average signal intensity and 95% confidence intervals each week, with individual signal intensity values shown in red and the total number of samples in which the drug was identified listed numerically. The horizontal axis label indicates the week in which the sample collection and analysis occurred, while the number in parenthesis indicates the number of samples that tested positive for at least one drug substance [Colour figure can be viewed at wileyonlinelibrary.com]

ethylamine (Figure 4a). Upon increasing the collision energy, however, further fragmentation of the initial m/z 266.1532 product yielded significant additional structural information (Figure 4b). As a starting point, product ions were annotated with their calculated molecular formula and corresponding neutral losses relative to the ion at m/z 266.1532. The base peak at m/z 155.0492, with a formula of $C_{11}H_7O^+$, was assigned as an acylium ion of naphthalene, with a corresponding ion at m/z 129.0700 resulting from the loss of CO. There is little ambiguity in these identifications as few stable ions could possess these formulas. The m/z 155.0492 ion and its neutral loss of $C_7H_{13}N$, inferred the presence of an amide group, with the naphthalene group on the C=O side. Further evidence for an amide was provided by the ion at m/z 58.0294, corresponding to $C_2H_4ON^+$,
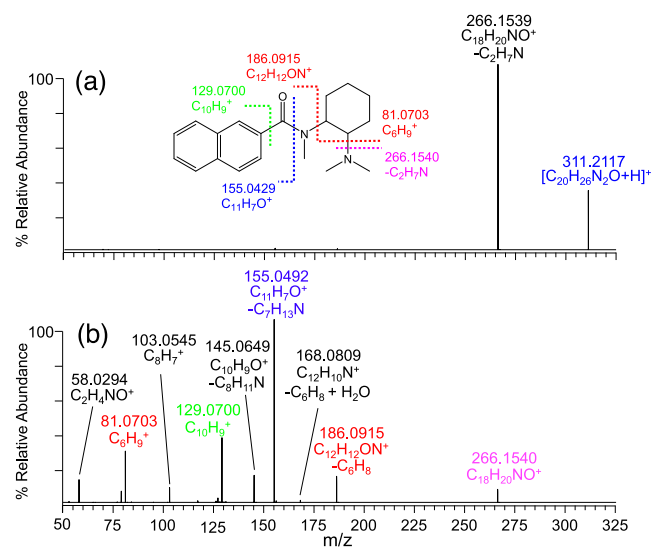
FIGURE 4 DART higher energy collision-induced dissociation tandem mass spectrometry (HCD-MS/MS) of the *m/z* 311.2122 ion from Figure 1a at (a) "low" 15% and (b) "high" 35% normalized collision energies. Neutral losses in panel (b) are shown relative to the initial *m/z* 266.1539 ion. The inset structure in panel (a) shows the proposed cleavage sites for β-U10 [Colour figure can be viewed at wileyonlinelibrary.com]

likely to be *N*-methylamide. The ion at *m/z* 81.0703 was suspected to be a cyclohexyl moiety ($C_6H_9^+$), connected to the nitrogen of the amide, with a complimentary product ion at *m/z* 186.0915 supporting a cleavage between the nitrogen of the amide and the cyclohexyl ring. Several candidate structures generated from this information were entered into SciFinder, where using substructure and similarity searches, a compound termed U10 (i.e., *N*-[2-(dimethylamino) cyclohexyl]-*N*-methylnaphthalene-1-carboxamide [herein termed α-U10]), was retrieved from a report by Hsu et al.[52] Further searching located a monograph in the SWGDrug database[53] containing characterization data for α-U10 including GC–MS, NMR, and FT-IR, but no ESI-MS/MS spectrum.

α-U10 and its *N*-[2-(dimethylamino)cyclohexyl]-*N*-methylnaphthalene-2-carboxamide (i.e., β-U10) isomer, first described by the Upjohn Company in the 1970s,[12] are structural analogs of the well-known "U-series" of synthetic *N,N*-dimethylcyclohexylbenzamide drugs, for which U-47700 has been widely reported as being responsible for, or contributing to, numerous deaths around the world.[14,54–57] Since 2017, when U-47700 was first subjected to regulatory controls, a range of additional structurally related compounds have appeared in the illicit drug market.[58] A comparison of the available MS/MS spectra for U-47700,[59] and other U-47700 analogs such as 3,4-methylenedioxy U-47700[60] against the MS/MS spectrum in Figure 4 revealed fragmentation patterns that were homologous with the expected fragmentation and structures of the α-U10 or β-U10 isomers, albeit not being able to distinguish one from the other.

The U-series of *N,N*-dimethylcyclohexylbenzamide drugs have isomeric counterparts assigned as AH- (or A-), originating from the

Allen and Hanburys company in the 1970s.[10] U-47700 and AH-7921 are the most well-known isomeric pair.[15] Although both families of drugs belong to the *N,N*-dimethylcyclohexylbenzamide class, there are key differences in their structures. U-series compounds have a 1,2-substituent arrangement on the cyclohexyl ring, whereas AH-series compounds have a geminal (1,1) configuration. For U-series compounds the *N*-methylamide nitrogen is bonded directly to a carbon on the cyclohexyl ring, while AH-series compounds bridge the amide nitrogen to the cyclohexyl ring via a methylene group. These structural differences give rise to different fragmentation behaviors such that the MS/MS spectra of U-47700 and AH-7921 can be readily differentiated from each other.[54,59] For example, for U-series compounds, a product ion at 81.0703 *m/z* is observed, corresponding to $C_6H_9^+$, whereas AH-series compounds show an analogous ion 14 Da higher at *m/z* 95.0861, corresponding to $C_7H_{11}^+$, the cyclohexyl moiety incorporating the methylene group. Furthermore, U-series compounds give a product ion at *m/z* 58.0294, corresponding to the methylamide fragment. This dissimilarity in fragmentation with AH-7921 allowed us to rule out the presence of "A10" isomers in the sample encountered here.[61]

In many of the samples where the *m/z* 311.2122 β-U10 ion was observed, another ion at *m/z* 298.1797 was also present, with a predicted molecular formula of $C_{19}H_{23}NO_2$ (calc. $[M + H]^+$ 298.1802). An example DART-MS spectrum obtained by trace residue sampling of a ziplock bag also containing heroin, xylitol, and β-U10, along with the HCD-MS/MS spectrum of the *m/z* 298.1797 ion, is shown in Figure S5. On the basis of the predicted molecular formula, and the fragmentation similarity with U10 seen in Figure 4, we propose this to be the protonated ester analog of β-U10, potentially formed as a by-product when synthesis of *N,N,N′*-trimethyl-1,2 diaminocyclohexane, a key precursor involved in β-U10 synthesis proceeded through a 2-dimethylaminocyclohexanol intermediate using the same process outlined in the patent from the Upjohn Company,[12] or an analogous pathway.

3.4 | Validation of the DART-MS results, synthesis of authentic reference standards, and GC–MS and LC–MS analysis for definitive identification and differentiation of the α-U10 and β-U10 isomers

Several of the samples collected in this study contained sufficient visible residue to enable their extraction and analysis using GC–MS. For example, in the sample whose DART-MS spectra were shown in Figure 1d, observed the week of September 21, 2020, a pale brown-colored visible residue was present in the metal tray. This tray was subsequently extracted with methanol and subjected to GC–MS analysis (Figure S6). With the exception of diphenhydramine that was not observed due to its thermal lability, the substances observed by GC–MS were consistent with those observed by DART-MS, including xylitol and heroin, and several other opioids present in raw opium including codeine, noscapine (identified by its thermal degradation product meconin), and papaverine,[62,63] as well as synthesis or degradation

products associated with heroin including acetylcodeine,[64] 6-monoacetylmorphine, and morphine (Figure S6a). In addition, a species eluting at 17.550 min, resulting in the electron ionization (EI)-MS spectrum shown in Figure S6b, was consistent with the reference spectrum for α-U10 in the SWGDrug monograph.[53] However, to determine if this corresponded to the α-U10 and/or β-U10 isomer, reference standards of both isomers were synthesized and then characterized as their freebase forms via X-ray crystallography (Figure S1) Note that reference standards for both isomers are now available from Cayman Chemical, sold under the name 1-naphthoyl U-47700 and 2-napthoyl U-47700, but were not available at the time of this work. GC–MS analysis of these standards using the same conditions as for the sample shown in Figure S6 resulted in a retention time for α-U10 of 17.161 and 17.518 min for β-U10, consistent with the retention time of 17.550 min for the sample, thereby confirming its identity as β-U10. Additional confirmation was provided via LC–MS analysis, where the sample eluted at the same retention time as the β-U10 standard (7.66 min), whereas the α-U10 isomer eluted at 8.32 min. GC–MS and/or LC–MS analysis of multiple other DDP samples collected at different time points and in which visible residue was present, all provided results consistent with those observed by DART-MS, and confirmed that only β-U10 was present throughout this pilot study. Notably, the results reported here for identification and characterization of β-U10, and the absence of the α-U10 isomer, are entirely consistent with those reported in July 2021 by Collins et al., who described the identification of β-U10 in Australia through the analysis of samples seized by law enforcement agencies in December 2020,[65] that is, several months after it was first observed in the study now reported here. The presence of β-U10 has since also been reported in Ohio, USA, in May 2021 under the name 2-naphthoyl U-47700.[66]

Minimal information regarding the pharmacological properties of β-U10 is available in the literature. The United States Patent 4,215,144, where this compound was first described, states "This invention relates to N-(2-aminocycloaliphatic)-benzamides and naphthamides that have been found to be useful for relieving pain in animals,"[12] suggesting that during their studies the compound may have been found to exhibit some activity. U-47700 is a potent μ-opioid receptor agonist, approximately 7.5 times more potent than morphine.[67] However, Hsu et al., who investigated a range of U- and A-series compounds interacting with human μ-opioid receptor 1 expressing cells,[52] reported that α-U10 had no observable agonistic effects. Szmuszkovicz reported that conversion of benzamides to acetamides resulted in reduced μ-receptor activity while still retaining analgesic properties, leading to the observation that the modification may result in increased selectivity for the κ-receptor.[67] This was termed the "eastern methylene group" effect. Subsequent studies of U-69593[68] and U-50488 confirmed this κ-selectivity.[69] Finally, Halfpenny et al. reported that several naphthalene derivatives of (+/−)-trans-N-methyl-N-[2-(1-pyrrolidinyl)cyclohexyl] benzo [b]thiophene-4-acetamide monohydrochloride (1,PD117302), which is an analog of U50,488, have high κ-opioid receptor affinity, selectivity, and potency.[70] This suggests that β-U10 may have selectivity and activity via the κ-opioid receptor. However, this remains to be determined.

3.5 | 213-nm photodissociation-MS/MS for differentiation of α-U10 and β-U10 isomers without need for chromatographic separation

Notably, the EI spectra obtained by GC–MS of the isomeric α-U10 and β-U10 reference standards, and the spectra obtained from the isomers using conventional HCD-MS/MS, were virtually indistinguishable from each other. For example, aside from a small difference in the ratio of product ions at m/z 126.1274 and m/z 127.0539 ions, corresponding to $C_8H_{16}N^+$ and $C_{10}H_7^+$ respectively, no unique product ions were observed for either species via HCD-MS/MS (Figures S7a and S7b, respectively). This suggests a necessity for chromatographic separation prior to MS analysis, not only for the characterization of novel drug substances but also to provide definitive identifications when multiple isomeric species may be present. This requirement, however, may limit throughput capacity for applications involving high throughput "street-level" drug monitoring, or where close to real time reporting is desired (particularly in field-based applications), due to the need to perform sample extraction prior to analysis and the relatively long timescales required for chromatographic analysis compared with using DART-MS. However, a range of alternate ion-activation/dissociation techniques have been developed in recent years, including UVPD, that provide access to fragmentation pathways not accessed using conventional collisional activated MS/MS methods and that enable "near complete" structural characterization for a wide range of biomolecules including peptides, proteins, protein post-translational modifications (PTMs), and lipids, including for isomeric species, without need for chromatographic separations.[71] To date, however, the potential utility of UVPD-MS/MS for the isomeric structural elucidation or differentiation of pharmaceutical or illicit drug species has not been explored.

Here, 213-nm UVPD-MS/MS of α-U10 and β-U10 using a commercially available mass spectrometry platform resulted in formation of the same products as observed using conventional HCD-MS/MS along with a number of unique, albeit low relative abundance, product ions for both isomers (Figure 5). For example, the α-U10 isomer yielded a unique ion at m/z 169.0519 ($C_{11}H_7NO^+$), corresponding to sequential cleavages of the cyclohexylamine and methylamine N-C bonds (Figure 5a), whereas the β-U10 isomer (Figure 5a) gave three unique ions, namely m/z 238.1584 corresponding to the combined losses of CO and N (CH$_3$)$_2$, m/z 198.0909 (loss of $C_7H_{15}N$) and m/z 169.0641 ($C_{12}H_9O^+$). These differences in fragmentation likely arise due to the 1- versus 2-naphthoyl substituted positions of the cyclohexylamide groups in the α-U10 and β-U10 isomers, and also that the N-methylamide bond in the α-U10 isomer adopted a trans-configuration while the β-U10 isomer adopted a cis-configuration (see Figure S1). These unique UVPD product ions, acquired using activation timescales and dissociation efficiencies similar to those used in conventional MS/MS strategies, clearly allow for the differentiation of these two isomers without the need for chromatographic separation. Therefore, UVPD has potential utility as a powerful new tool for the enhanced identification and analysis of novel illicit drug substances.
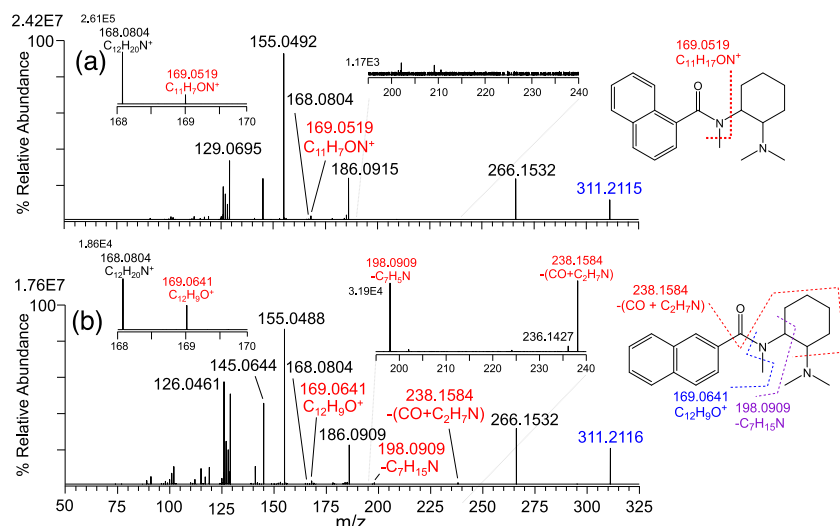
FIGURE 5 213-nm ultraviolet photodissociation tandem mass spectrometry (UVPD-MS/MS) of (a) α-U10 and (b) β-U10 synthetic reference standards. The insets in each panel show expanded regions of the spectra from *m/z* 168–170 and *m/z* 195–240. Unique product ions for each structure are highlighted in red. The inset structures show the proposed cleavage sites for the α-U10 and β-U10 isomers [Colour figure can be viewed at wileyonlinelibrary.com]

4 | CONCLUSIONS

The identification, characterization, and reporting of novel illicit drug substances are predominately achieved via the analysis of seized samples using conventional analytical and forensic chemistry methods such as GC–MS, LC–MS, and NMR. However, by the time this occurs, it is likely that a drug is already in widespread use within the community. Here, trace-residue analysis of DDP using DART-MS and MS/MS, combined with advanced MS/MS methods such as UPVD, is demonstrated to be a powerful alternate method for (i) large-scale identification and monitoring of illicit drugs and complex poly-drug combinations at the point closest to where drug consumption occurs, (ii) monitoring longitudinal changes in the number and/or ASI of a particular drug or poly-drug combination as proxy indicators of changes in market conditions over time, and (iii) the identification and characterization of novel drug substances including NSOs that have not previously been reported.

DATA AVAILABILITY STATEMENT

The data that support the findings of this study are available from the corresponding author upon reasonable request.

ORCID

Dimitri Gerostamoulos https://orcid.org/0000-0002-7958-8235
Gavin E. Reid https://orcid.org/0000-0002-9675-1444

REFERENCES

1. Bade R, Tscharke BJ, O'Brien JW, et al. Impact of COVID-19 Controls on the Use of Illicit Drugs and Alcohol in Australia. *Environ Sci Technol Lett*. 2021;8(9):799-804. doi:10.1021/acs.estlett.1c00532
2. Reinstadler V, Ausweger V, Grabher AL, et al. Monitoring drug consumption in Innsbruck during coronavirus disease 2019 (COVID-19) lockdown by wastewater analysis. *Sci Total Environ*. 2021;757:144006. doi:10.1016/j.scitotenv.2020.144006
3. Been F, Emke E, Matias J, et al. Changes in drug use in European cities during early COVID-19 lockdowns—a snapshot from wastewater analysis. *Environ Int*. 2021;153:106540. doi:10.1016/j.envint.2021.106540
4. Farhoudian A, Radfar SR, Mohaddes Ardabili H, et al. A global survey on changes in the supply, price, and use of illicit drugs and alcohol, and related complications during the 2020 COVID-19 pandemic. *Front Psych*. 2021;12:646206. doi:10.3389/fpsyt.2021.646206
5. Price O, Man N, Bruno R, et al. Changes in illicit drug use and markets with the COVID-19 pandemic and associated restrictions: findings from the Ecstasy and Related Drugs Reporting System, 2016-20. *Addiction*. 2022;117(1):182-194. doi:10.1111/add.15620
6. Solimini R, Pichini S, Pacifici R, Busardò FP, Giorgetti R. Pharmacotoxicology of non-fentanyl derived new synthetic opioids. *Front Pharmacol*. 2018;9:654. doi:10.3389/fphar.2018.00654
7. Mather LE. Clinical pharmacokinetics of fentanyl and its newer derivatives. *Clin Pharmacokinet*. 1983;8(5):422-446. doi:10.2165/00003088-198308050-00004
8. Armenian P, Vo KT, Barr-Walker J, Lynch KL. Fentanyl, fentanyl analogs and novel synthetic opioids: a comprehensive review. *Neuropharmacology*. 2018;134(Pt A):121-132. doi:10.1016/j.neuropharm.2017.10.016
9. Vardanyan RS, Hruby VJ. Fentanyl-related compounds and derivatives: current status and future prospects for pharmaceutical applications. *Future Med Chem*. 2014;6(4):385-412. doi:10.4155/fmc.13.215
10. Harper NJ, Veitch GB, Wibberley DG. 1-(3,4-Dichlorobenzamidomethyl)cyclohexyldimethylamine and related compounds as potential analgesics. *J Med Chem*. 1974;17(11):1188-1193. doi:10.1021/jm00257a012
11. Harper NJ, Veitch GBA. Ethylene diamine derivatives. 1977, US. Patent US4049663A.
12. Szmuszkovic J. Analgesic *N*-(2-[furylmethylamino and 2-thienylmethylamino]cycloaliphatic)benzamides. 1979, US. Patent US4153717A.
13. Baumann MH, Tocco G, Papsun DM, Mohr AL, Fogarty MF, Krotulski AJ. U-47700 and its analogs: non-fentanyl synthetic opioids

impacting the recreational drug market. *Brain Sci.* 2020;10(11):895. doi:10.3390/brainsci10110895

14. Coopman V, Blanckaert P, van Parys G, van Calenbergh S, Cordonnier J. A case of acute intoxication due to combined use of fentanyl and 3,4-dichloro-*N*-[2-(dimethylamino)cyclohexyl]-*N*-methylbenzamide (U-47700). *Forensic Sci Int.* 2016;266:68-72. doi:10.1016/j.forsciint.2016.05.001

15. Katselou M, Papoutsis I, Nikolaou P, Spiliopoulou C, Athanaselis S. AH-7921: the list of new psychoactive opioids is expanded. *Forensic Toxicol.* 2015;33(2):195-201. doi:10.1007/s11419-015-0271-z

16. Mohr AL, Friscia M, Papsun D, Kacinko SL, Buzby D, Logan BK. Analysis of novel synthetic opioids U-47700, U-50488 and furanyl fentanyl by LC-MS/MS in postmortem casework. *J Anal Toxicol.* 2016; 40(9):709-717. doi:10.1093/jat/bkw086

17. Breindahl T, Kimergård A, Andreasen MF, Pedersen DS. Identification of a new psychoactive substance in seized material: the synthetic opioid *N*-phenyl-*N*-[1-(2-phenethyl)piperidin-4-yl]prop-2-enamide (acrylfentanyl). *Drug Test Anal.* 2017;9(3):415-422. doi:10.1002/dta.2046

18. Blanckaert P, Balcaen M, Vanhee C, et al. Analytical characterization of "etonitazepyne," a new pyrrolidinyl-containing 2-benzylbenzimidazole opioid sold online. *Drug Test Anal.* 2021;13(9): 1627-1634. doi:10.1002/dta.3113

19. Verougstraete N, Vandeputte MM, Lyphout C, et al. First report on brorphine: the next opioid on the deadly new psychoactive substance horizon? *J Anal Toxicol.* 2021;44(9):937-946. doi:10.1093/jat/bkaa094

20. Néfau T, Charpentier E, Elyasmino N, Duplessy-Garson C, Levi Y, Karolak S. Drug analysis of residual content of used syringes: a new approach for improving knowledge of injected drugs and drug user practices. *Int J Drug Policy.* 2015;26(4):412-419. doi:10.1016/j.drugpo.2014.09.010

21. Fiorentin TR, Logan BK. Analytical findings in used syringes from a syringe exchange program. *Int J Drug Policy.* 2020;81:102770. doi:10.1016/j.drugpo.2020.102770

22. Lefrançois E, Augsburger M, Esseiva P. Drug residues in used syringes in Switzerland: A comparative study. *Drug Test Anal.* 2018;10(5):874-879. doi:10.1002/dta.2335

23. Lefrancois E, Belackova V, Silins E, et al. Substances injected at the Sydney supervised injecting facility: a chemical analysis of used injecting equipment and comparison with self-reported drug type. *Drug Alcohol Depend.* 2020;209:107909. doi:10.1016/j.drugalcdep.2020.107909

24. Brunt TM, Lefrançois E, Gunnar T, et al. Substances detected in used syringes of injecting drug users across 7 cities in Europe in 2017 and 2018: The European Syringe Collection and Analysis Project Enterprise (ESCAPE). *Int J Drug Policy.* 2021;95:103130. doi:10.1016/j.drugpo.2021.103130

25. Gozdzialski L, Aasen J, Larnder A, et al. Portable gas chromatography-mass spectrometry in drug checking: detection of carfentanil and etizolam in expected opioid samples. *Int J Drug Policy.* 2021;97:103409. doi:10.1016/j.drugpo.2021.103409

26. Dresen S, Ferreirós N, Gnann H, Zimmermann R, Weinmann W. Detection and identification of 700 drugs by multi-target screening with a 3200 Q TRAP LC-MS/MS system and library searching. *Anal Bioanal Chem.* 2010;396(7):2425-2434. doi:10.1007/s00216-010-3485-2

27. di Rago M, Pantatan S, Hargreaves M, et al. High throughput detection of 327 drugs in blood by LC-MS-MS with automated data processing. *J Anal Toxicol.* 2021;45(2):154-183. doi:10.1093/jat/bkaa057

28. Morelato M, Beavis A, Kirkbride P, Roux C. Forensic applications of desorption electrospray ionisation mass spectrometry (DESI-MS). *Forensic Sci Int.* 2013;226(1-3):10-21. doi:10.1016/j.forsciint.2013.01.011

29. Stojanovska N, Tahtouh M, Kelly T, Beavis A, Fu S. Qualitative analysis of seized cocaine samples using desorption electrospray ionization–mass spectrometry (DESI-MS). *Drug Test Anal.* 2015;7(5): 393-400. doi:10.1002/dta.1684

30. Vircks KE, Mulligan CC. Rapid screening of synthetic cathinones as trace residues and in authentic seizures using a portable mass spectrometer equipped with desorption electrospray ionization. *Rapid Commun Mass Spectrom.* 2012;26(23):2665-2672. doi:10.1002/rcm.6390

31. Vandergrift GW, Gill CG. Paper spray mass spectrometry: a new drug checking tool for harm reduction in the opioid overdose crisis. *J Mass Spectrom.* 2019;54(9):729-737. doi:10.1002/jms.4431

32. Vandergrift GW, Hessels AJ, Palaty J, Krogh ET, Gill CG. Paper spray mass spectrometry for the direct, semi-quantitative measurement of fentanyl and norfentanyl in complex matrices. *Clin Biochem.* 2018;54: 106-111. doi:10.1016/j.clinbiochem.2018.02.005

33. Borden SA, Saatchi A, Vandergrift GW, Palaty J, Lysyshyn M, Gill CG. A new quantitative drug checking technology for harm reduction: pilot study in Vancouver, Canada using paper spray mass spectrometry. *Drug Alcohol Rev.* 2022;41(2):410-418. doi:10.1111/dar.13370

34. Jackson AU, Garcia-Reyes JF, Harper JD, et al. Analysis of drugs of abuse in biofluids by low temperature plasma (LTP) ionization mass spectrometry. *Analyst.* 2010;135(5):927-933. doi:10.1039/b920155f

35. McCullough BJ, Patel K, Francis R, et al. Atmospheric solids analysis probe coupled to a portable mass spectrometer for rapid identification of bulk drug seizures. *J Am Soc Mass Spectrom.* 2020;31(2):386-393. doi:10.1021/jasms.9b00020

36. Grange AH, Sovocool GW. Detection of illicit drugs on surfaces using direct analysis in real time (DART) time-of-flight mass spectrometry. *Rapid Commun Mass Spectrom.* 2011;25(9):1271-1281. doi:10.1002/rcm.5009

37. Sisco ER, Verkouteren JR, Staymates JL, Lawrence JA. Rapid detection of fentanyl, fentanyl analogues, and opioids for on-site or laboratory based drug seizure screening using thermal desorption DART-MS and ion mobility spectrometry. *Forensic Chem.* 2017;4:108-115. doi:10.1016/j.forc.2017.04.001

38. Sisco E, Robinson EL, Burns A, Mead R. What's in the bag? Analysis of exterior drug packaging by TD-DART-MS to predict the contents. *Forensic Sci Int.* 2019;304:109939. doi:10.1016/j.forsciint.2019.109939

39. Brown H, Oktem B, Windom A, Doroshenko V, Evans-Nguyen K. Direct analysis in real time (DART) and a portable mass spectrometer for rapid identification of common and designer drugs on-site. *Forensic Chem.* 2016;1:66-73. doi:10.1016/j.forc.2016.07.002

40. West H, Fitzgerald J, Hopkins K, et al. Early warning system for illicit drug use at large public events: trace residue analysis of discarded drug packaging samples. *J Am Soc Mass Spectrom.* 2021;32(10): 2604-2614. doi:10.1021/jasms.1c00232

41. Nan Q, Hejian W, Ping X, et al. Investigation of fragmentation pathways of fentanyl analogues and novel synthetic opioids by electron ionization high-resolution mass spectrometry and electrospray ionization high-resolution tandem mass spectrometry. *J Am Soc Mass Spectrom.* 2020;31(2):277-291. doi:10.1021/jasms.9b00112

42. Moorthy AS, Kearsley AJ, Mallard WG, Wallace WE. Mass spectral similarity mapping applied to fentanyl analogs. *Forensic Chem.* 2020; 19:100237. doi:10.1016/j.forc.2020.100237

43. Davidson JT, Piacentino EL, Sasiene ZJ, et al. Identification of novel fragmentation pathways and fragment ion structures in the tandem mass spectra of protonated synthetic cathinones. *Forensic Chem.* 2020;19:100245. doi:10.1016/j.forc.2020.100245

44. Sekuła K, Wrzesień-Tokarczyk W, Stanaszek R, Byrska B, Zuba D. Analysis of fragmentation pathways of fentanyl derivatives by electrospray ionisation high-resolution mass spectrometry. *Rapid Commun Mass Spectrom.* 2022;13(7):e9254. doi:10.1002/rcm.9254

45. https://www.npsdiscovery.org/reports/monographs/

46. Adusumilli R, Mallick P. Data conversion with proteowizard msconvert. *Methods Mol Biol*. 2017;1550:339-368. doi:10.1007/978-1-4939-6747-6_23

47. Bald T, Barth J, Niehues A, Specht M, Hippler M, Fufezan C. pymzML—Python module for high-throughput bioinformatics on mass spectrometry data. *Bioinformatics*. 2012;28(7):1052-1053. doi:10.1093/bioinformatics/bts066

48. Sheldrick GM. Crystal structure refinement with SHELXL. *Acta Crystallogr C*. 2015;71(1):3-8. doi:10.1107/S2053229614024218

49. Macrae CF, Bruno IJ, Chisholm JA, et al. Mercury CSD 2.0—new features for the visualization and investigation of crystal structures. *J Appl Cryst*. 2008;41(2):466-470. doi:10.1107/S0021889807067908

50. Farrugia LJ. WinGX suite for small-molecule single-crystal crystallography. *J Appl Cryst*. 1999;32(4):837-838. doi:10.1107/S0021889899006020

51. Nielsen S, McAuley A. Etizolam: a rapid review on pharmacology, non-medical use and harms. *Drug Alcohol Rev*. 2020;39(4):330-336. doi:10.1111/dar.13052

52. Hsu T, Mallareddy JR, Yoshida K, et al. Synthesis and pharmacological characterization of ethylenediamine synthetic opioids in human μ-opiate receptor 1 (OPRM1) expressing cells. *Pharmacol Res Perspect*. 2019;7(5):e00511. doi:10.1002/prp2.511

53. https://swgdrug.org/Monographs/U10.pdf

54. Kronstrand R, Thelander G, Lindstedt D, Roman M, Kugelberg FC. Fatal intoxications associated with the designer opioid AH-7921. *J Anal Toxicol*. 2014;38(8):599-604. doi:10.1093/jat/bku057

55. Fels H, Lottner-Nau S, Sax T, et al. Postmortem concentrations of the synthetic opioid U-47700 in 26 fatalities associated with the drug. *Forensic Sci Int*. 2019;301:e20-e28. doi:10.1016/j.forsciint.2019.04.010

56. Kraemer M, Boehmer A, Madea B, Maas A. Death cases involving certain new psychoactive substances: a review of the literature. *Forensic Sci Int*. 2019;298:186-267. doi:10.1016/j.forsciint.2019.02.021

57. Elliott SP, Brandt SD, Smith C. The first reported fatality associated with the synthetic opioid 3,4-dichloro-*N*-[2-(dimethyl amino) cyclohexyl]-*N*-methylbenzamide (U-47700) and implications for forensic analysis. *Drug Test Anal*. 2016;8(8):875-879. doi:10.1002/dta.1984

58. Sharma KK, Hales TG, Rao VJ, NicDaeid N, McKenzie C. The search for the "next" euphoric non-fentanil novel synthetic opioids on the illicit drugs market: current status and horizon scanning. *Forensic Toxicol*. 2019;37(1):1-16. doi:10.1007/s11419-018-0454-5

59. Fleming SW, Cooley JC, Johnson L, et al. Analysis of U-47700, a novel synthetic opioid, in human urine by LC-MS-MS and LC-QToF. *J Anal Toxicol*. 2017;41(3):173-180. doi:10.1093/jat/bkw131

60. Poplawska M, Bednarek E, Naumczuk B, Kozerski L, Błażewicz A. Identification and structure characterization of five synthetic opioids: 3,4-methylenedioxy-U-47700, o-methyl-acetylfentanyl, 2-thiophenefentanyl, benzoylfentanyl and benzoylbenzylfentanyl. *Forensic Toxicol*. 2021;39(1):45-58. doi:10.1007/s11419-020-00539-6

61. https://www.swgdrug.org/Monographs/A10%20HCl.pdf

62. Paterson S, Cordero R. Comparison of the various opiate alkaloid contaminants and their metabolites found in illicit heroin with 6-monoacetyl morphine as indicators of heroin ingestion. *J Anal Toxicol*. 2006;30(4):267-273. doi:10.1093/jat/30.4.267

63. Bogusz MJ, Maier RD, Erkens M, Kohls U. Detection of non-prescription heroin markers in urine with liquid chromatography-atmospheric pressure chemical ionization mass spectrometry. *J Anal Toxicol*. 2001;25(6):431-438. doi:10.1093/jat/25.6.431

64. O'Neal CL, Poklis A, Lichtman AH. Acetylcodeine, an impurity of illicitly manufactured heroin, elicits convulsions, antinociception, and locomotor stimulation in mice. *Drug Alcohol Depend*. 2001;65(1):37-43. doi:10.1016/S0376-8716(01)00145-4

65. Collins M, Brown D, Davies S, et al. Case study: identification and characterization of *N*-[2-(dimethylamino)cyclohexyl]-*N*-methylnaphthalene-2-carboxamide, a regioisomer of the synthetic opioid U10. *Drug Test Anal*. 2022;14(1):188-195. doi:10.1002/dta.3133

66. https://www.nflis.deadiversion.usdoj.gov/nflisdata/docs/NFLIS_Synth-Opioids_2-naphthyl_U47700.pdf

67. Szmuszkovicz J, von Voigtlander PF. Benzeneacetamide amines: structurally novel non-mμ opioids. *J Med Chem*. 1982;25(10):1125-1116. doi:10.1021/jm00352a005

68. la Regina A, Petrillo P, Sbacchi M, Tavani A. Interaction of U-69,593 with mu-, alpha- and kappa-opioid binding sites and its analgesic and intestinal effects in rats. *Life Sci*. 1988;42(3):293-301. doi:10.1016/0024-3205(88)90638-8

69. Vonvoigtlander PF, Lahti RA, Ludens JH. U-50,488: a selective and structurally novel non-Mu (kappa) opioid agonist. *J Pharmacol Exp Ther*. 1983;224(1):7-12.

70. Halfpenny PR, Horwell DC, Hughes J, et al. Highly selective kappa opioid analgesics. 4. Synthesis of some conformationally restricted naphthalene derivatives with high receptor affinity and selectivity. *J Med Chem*. 1991;34(1):190-194. doi:10.1021/jm00105a028

71. Brodbelt JS, Morrison LJ, Santos I. Ultraviolet photodissociation mass spectrometry for analysis of biological molecules. *Chem Rev*. 2020;120(7):3328-3380. doi:10.1021/acs.chemrev.9b00440

SUPPORTING INFORMATION

Additional supporting information may be found in the online version of the article at the publisher's website.